Journal of Alloys and Compounds 509 (2011) 8441–8448

Contents lists available at ScienceDirect

Journal of Alloys and Compounds

journal homepage: www.elsevier.com/locate/jallcom

Suppressing effect of 0.5 wt.% nano-TiO_2 addition into Sn–3.5Ag–0.5Cu solder alloy on the intermetallic growth with Cu substrate during isothermal aging

L.C. Tsao*

Department of Materials Engineering, National Pingtung University of Science & Technology, 1, Hseuhfu Road, Neipu, 91201 Pingtung, Taiwan

ARTICLE INFO

Article history:
Received 14 December 2010
Received in revised form 30 May 2011
Accepted 31 May 2011
Available online 15 June 2011

Keywords:
Composite solder
Sn3.5Ag0.5Cu
TiO_2 nanoparticles
Isothermal aging

ABSTRACT

This study investigated the effects of adding 0.5 wt.% nano-TiO_2 particles into Sn3.5Ag0.5Cu (SAC) lead-free solder alloys on the growth of intermetallic compounds (IMC) with Cu substrates during solid-state isothermal aging at temperatures of 100, 125, 150, and 175 °C for up to 7 days. The results indicate that the morphology of the Cu_6Sn_5 phase transformed from scallop-type to layer-type in both SAC solder/Cu joints and Sn3.5Ag0.5Cu–0.5 wt.% TiO_2 (SAC) composite solder/Cu joints. In the SAC solder/Cu joints, a few coarse Ag_3Sn particles were embedded in the Cu_6Sn_5 surface and grew with prolonged aging time. However, in the SAC composite solder/Cu aging, a great number of nano-Ag_3Sn particles were absorbed in the Cu_6Sn_5 surface. The morphology of adsorption of nano-Ag_3Sn particles changed dramatically from adsorption-type to moss-type, and the size of the particles increased.

The apparent activation energies for the growth of overall IMC layers were calculated as 42.48 kJ/mol for SAC solder and 60.31 kJ/mol for SAC composite solder. The reduced diffusion coefficient was confirmed for the SAC composite solder/Cu joints.

1. Introduction

Recently, many different solder alloys have been proposed as potential replacements for Pb-free solder. The European Union directive on waste electrical and electronic equipment (WEEE) announced the prohibition of the use of Pb in the consumer electronics market after January 2006. Among several candidate alloys, the Sn–Ag–Cu solder (SAC) family is believed to be the most promising. Sn–Ag–Cu solder has been proposed as the most promising substitute for lead-containing solders because of its relatively low melting temperature, its superior mechanical properties, and its relatively good wettability [1–3]. However, during the soldering process, the metallurgical reaction between liquid solder and copper or Ni/Au metallization results in an intermetallic compound (IMC) layer at the joint interface. Thick IMC growth may have a deleterious effect [4–6]. Thick intermetallic growth degrades the joining property, due to the brittle nature of the IMC and the mismatches in physical properties, such as the thermal expansion coefficient and elastic modulus. Excessive thickness may also decrease solder joint ductility and strength [7]. Recently, composite solders have been identified as potential materials that may provide higher strength as compared to conventional solders [8–13]. In particular, the addition of dioxide nanopowders enhances the strength of the solder. Tsao and Chang added TiO_2 nanoparticles to Sn3.5Ag0.25Cu lead-free solder alloys [10]. The mechanical properties (microhardness, 0.2%YS, and UTS) improved as a result. Tsao et al. added nanopowders of Al_2O_3 to a conventional SAC solder [11]. Microhardness was improved by the addition the nanopowders. This improvement in the mechanical property was due to the composite microstructure, which was close to the theoretical prediction from dispersion strengthening theory. Moreover, the composite solder joints apparently decreased the surface energy and hindered the growth of the Cu6Sn5 IMC layer [12,13]. Shen et al. [14] investigated the Sn–3.5Ag–ZrO_2 composite solders and found that the primary β-Sn dendrites and Ag_3Sn phases were refined.

However, an evaluation of the growth kinetics of the interfacial reaction between Sn–Ag–Cu solder and Cu substrate during solid-state aging has not been sufficiently performed.

The literature contains many studies on Sn-based composite solder alloys, such as microstructures, mechanical properties, and interfacial reactions [8–14]. However, information on the growth kinetics of Cu–Sn IMC at the SAC composite solder/Cu interface during solid-state aging is scarce. This study focuses on the kinetics of the Cu–Sn IMC growth for the Sn3.5Ag0.5Cu composite solder/Cu system during solid-state aging. Also, the activation energy of the IMC growth was determined from the temperature dependence of the square of the layer growth rate.

* Tel.: +886 8 7703202x7560; fax: +886 8 7740552.
E-mail address: tlclung@mail.npust.edu.tw

0925-8388/$ – see front matter © 2011 Elsevier B.V. All rights reserved.
doi:10.1016/j.jallcom.2011.05.116

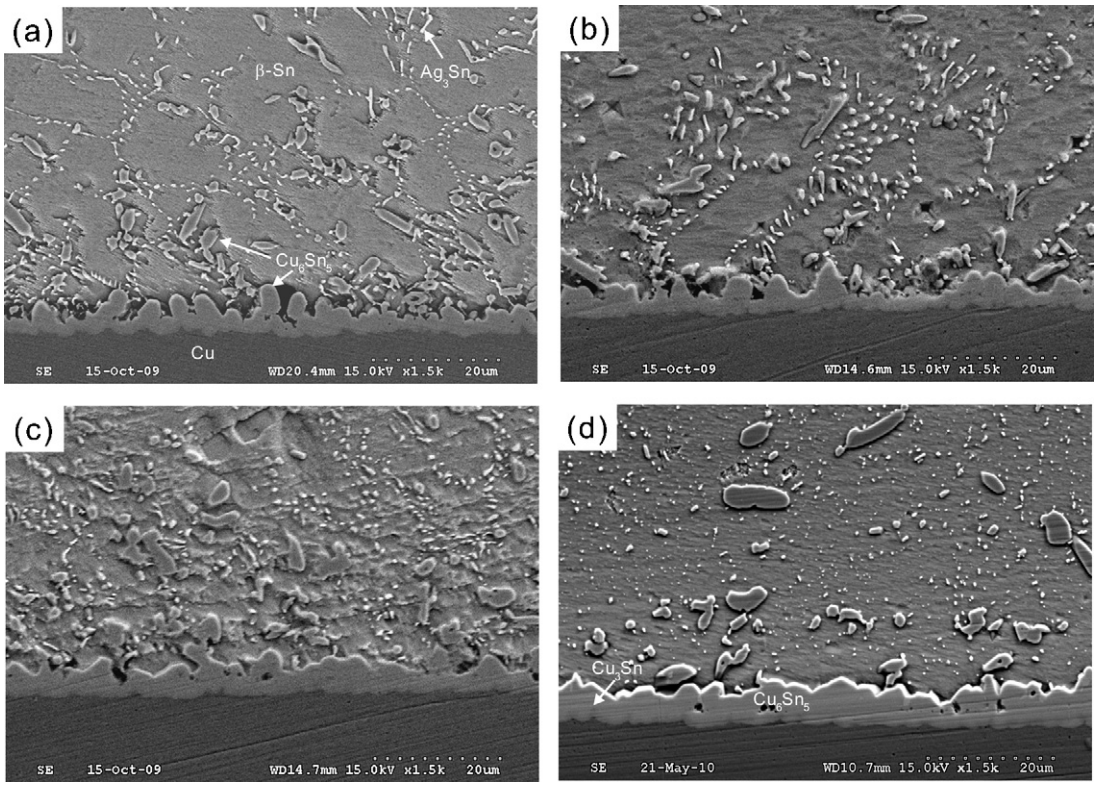

Fig. 1. Cross-section SEM images of the SAC solder/Cu interfaces aged at 175 °C for the following times: (a) as-reflowing; (b) 0.5 day; (c) 2 days; and (d) 7 days.

2. Experimental procedures

The SAC composite solders were prepared via mechanically incorporating 0.5 wt.% of about 20 nm TiO_2 nanopowders (Nanostructured & Amorphous materials, USA) into the Sn3.5Ag0.5Cu solder (SAC, Shenmao Technology, Inc., Taiwan) paste, with subsequent remelting in a vacuum furnace at 650 °C for 2.5 h and casting in a mold. The solder was melted in a crucible and chill cast in a water-cooled copper mold to form square ingots of 8 mm × 10 mm × 20 mm. Then the solder was cold-rolled and a disk-type specimen (6 mm in diameter, 0.9 g) punched out.

The substrates used in this study were pure Cu sheets measuring 10 mm × 10 mm × 1 mm. These Cu substrates were cleaned with acetone and etched in a 10% H_2SO_4–90% CH_3OH solution to remove surface oxides and contaminants. The SAC composite solder/Cu joint samples were prepared by reflowing the solder on the Cu substrates. Solder sheets and Cu plates were ultrasonically cleaned in ethanol before soldering. Rosin mildly activated (RMA) flux was used in this test. The substrates were heated on a hot plate to 30 °C above the melting temperature of the solder, and the temperature was kept stable, within ±3 °C.

Each reaction couple was then placed in an oven maintained at a constant aging temperature. Accelerated aging was performed in air furnaces with a temperature control of ±0.5 °C. The aging temperatures were 100, 125, 150, and 175 °C. The time periods were 0.5–7 days, with a tracking error of ±30 min.

For observation of the morphologies of the IMC formed at the SAC composite solder/Cu interface after aging reactions, the unreacted solder covering the scallops was removed by mechanical polishing, followed by selective chemical etching. The selective etching solution was composed of 1 part nitric acid, 1 part acetic acid, and 4 parts glycerol. The morphologies were studied using a scanning electron microscope (SEM, s-3000H, Hitachi Co.) with a voltage of 20 keV. X-ray diffraction (XRD, D/max 2500 V/PC) and energy dispersive spectroscopy (EDS) were used to analyze the composition. For Ag_3Sn grain size analysis, the size of the Ag_3Sn grains was calculated with the *Image-Pro* software, and the average values were calculated based on these data.

The polished cross sections of the solder/substrate diffusion couples were examined by SEM, and the digitally captured micrographs were semi-automatically processed using the *Image-Pro* software to determine the average thickness (x) of the intermetallic layer. Five micrographs were used for each interdiffusion experimental condition. The average thickness of the IMC layer (x) was calculated by using the following equation:

$$x = \frac{S}{L} \tag{1}$$

where L is the length measured, and S is the integral contour area of the intermetallic layer at the interface.

3. Results and discussion

3.1. Evolutions of the IMC at the interface

Figs. 1 and 2 show the microstructural evolutions of the SAC solder/Cu interface after aging. It can be seen in Fig. 1a that a continuous scallop-type IMC layer formed at the solder/Cu interface during the initial soldering (no aging). In the as-soldered joints, the Cu_6Sn_5 IMC located at the SAC solder/Cu interface was identified by means of EDS analysis, and the thickness of the IMC was approximately 2.2 μm. However, no Cu_3Sn IMC was found, as shown in Fig. 1a. According to the Cu–Sn phase diagram, Cu_6Sn_5 and Cu_3Sn are the main reaction products below about 350 °C. Although Cu_3Sn was not observed at the low temperatures, Cu_3Sn is known to form during soldering, based on previous TEM study of the Sn–Ag–Bi solder/Cu system [15]. However, the Cu_3Sn layer was probably not observed in samples with short soldering times and low temperatures due to the limited spatial resolution of the SEM.

In addition, accompanying the formation of the IMC in the solder matrix, Ag_3Sn appeared at the grain boundary, and coarse Cu–Sn IMC appeared in the matrix. After isothermal aging at 175 °C, the SAC solder/Cu interface exhibited a duplex structure of Cu_6Sn_5 and Cu_3Sn IMC, as shown in Fig. 2b and c. Moreover, the morphology of the IMC layer changed from an uneven scallop-type to a layer-type with prolonged aging. A similar result was also reported by Tu and Thompson [16]. They reported on the phase transformation of Cu_3Sn to Cu_6Sn_5 with increased aging temperature, and reported that Cu_3Sn formed and grew at higher temperature (115–150 °C).

The thickness of the overall IMC layer increased greatly with higher aging temperatures and prolonged aging time (Figs. 1 and 2). When the aging time was prolonged to 7 days, the large number of Ag_3Sn IMC was reduced further, while a change in the morphology of Ag_3Sn IMC was found, as seen in Fig. 2.

Figs. 3 and 4 show the microstructural evolutions of the SAC composite solder/Cu interface after reflowing. It is clearly shown

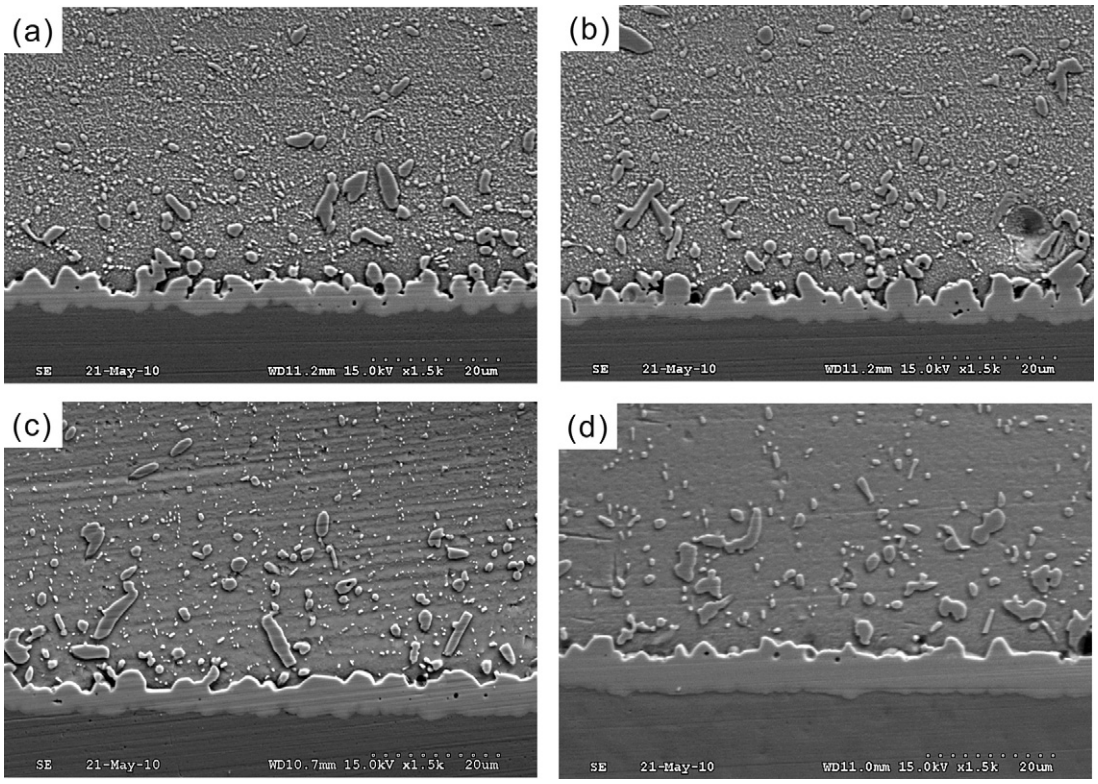

Fig. 2. Cross-section SEM images of the SAC solder/Cu interfaces aged for 7 days at different temperatures: (a) 100 °C; (b) 125 °C; (c) 150 °C; and (d) 175 °C.

in Fig. 3a that a discontinuous scallop-type Cu_6Sn_5 IMC layer formed at the SAC composite solder/Cu interface after the reflowing process. In addition, a large number of dot-shaped Ag_3Sn precipitates and the Cu_6Sn_5 IMC did not appear in the solder matrix in the SAC composite solder joints, as shown in Fig. 3a. This morphology is different from that of the SAC solder (Fig. 1a). This difference in morphology indicates that the nano-TiO_2 particles had a significant effect on the observed phenomenon,

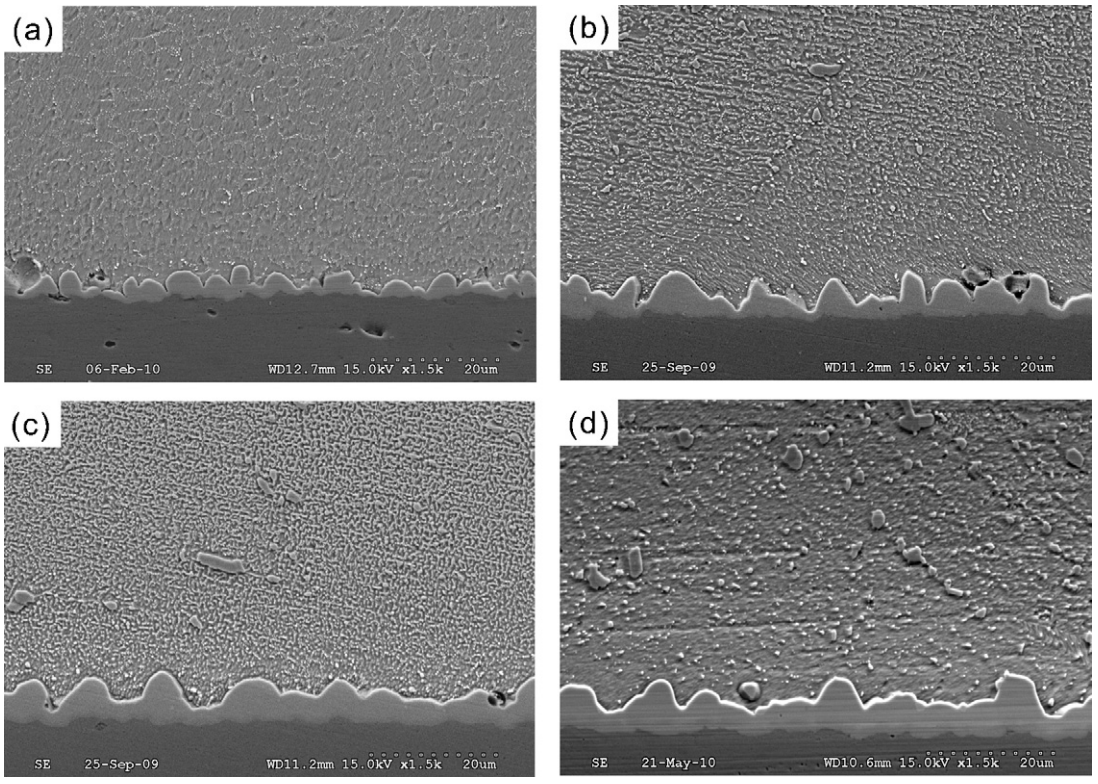

Fig. 3. Cross-section SEM images of the SAC composite solder/Cu interfaces aged at 175 °C for the following times: (a) as-reflowing; (b) 0.5 day; (c) 2 days; and (d) 7 days.

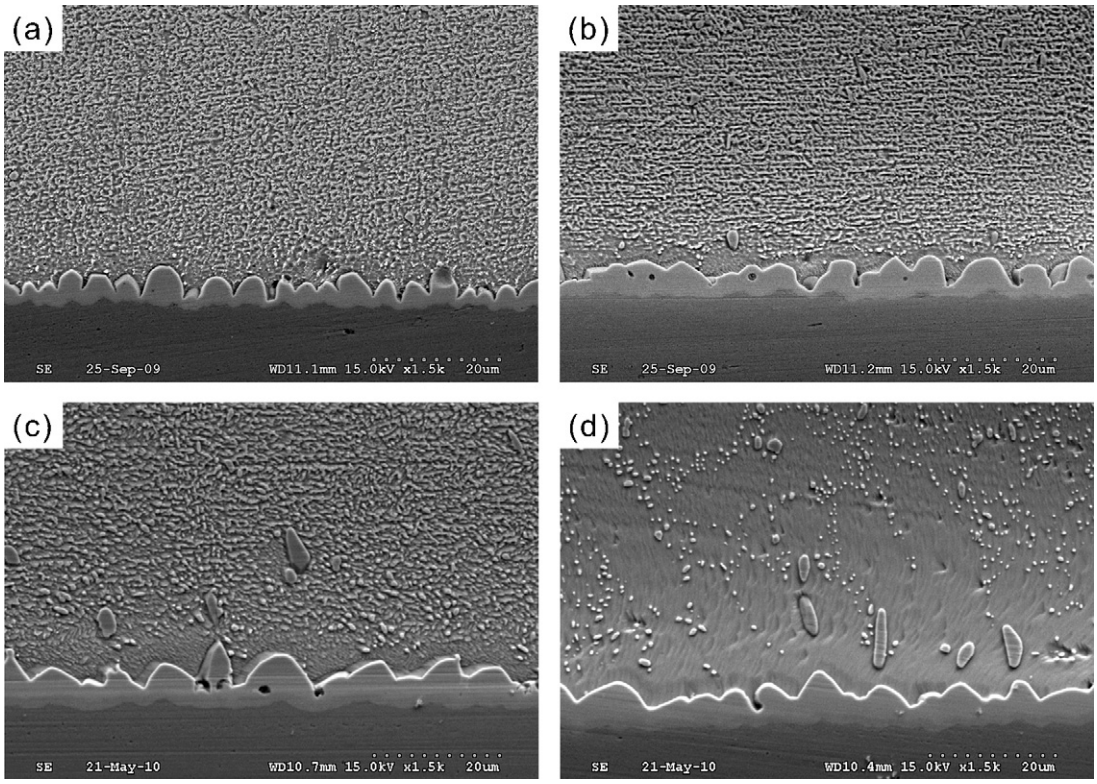

Fig. 4. Cross-section SEM images of the SAC composite solder/Cu interfaces aged for 7 days at different temperatures: (a) 100 °C; (b) 125 °C; (c) 150 °C; and (d) 175 °C.

and a reasonable explanation for this will be provided in detail below.

After 7 days of aging, it was found that the IMC layer at the interface had, overall, gradually transformed from the discontinuous scallop-type to the layer-type in the SAC composite solder joints (Figs. 3 and 4). In addition, the old precipitated Ag_3Sn IMC grew, and new Cu_6Sn_5 particles continued to appear for 7 days in the SAC composite joints, as can be seen in Fig. 4. In the SAC composite solder joints, in terms of morphology, the precipitated Ag_3Sn IMC gradually transformed from floc to graininess along with prolonged aging time. Also, because the Ag_3Sn IMC in SAC composite solder joints varied greatly in size, the large Ag_3Sn IMC will easily consume the small ones adjacent to them, forming even larger ones. This observed phenomenon is remarkable in comparison to that in SAC composite solder joints. For SAC composite solder joints, the precipitated Ag_3Sn still had a uniform size and even distribution in the solder matrix. A similar result was also reported by Hao et al. [17].

As aforementioned, the nano-TiO_2 particle additive could play an important role in refining the Ag_3Sn IMC in the solder matrix in reflowing. The proposed mechanism of this refinement can be summarized as follows: During the reflow process, nano-TiO_2 particles are dispersed in the molten solder and are much smaller than those of the Ag_3Sn IMC. The nano-TiO_2 particles cling to the Ag_3Sn IMC, just as spheres cling to a plane. To simplify the analysis, we treat the Ag_3Sn crystal surface as a plane and the nano-TiO_2 particles as spheres. So, the theory of adsorption of a surface-active material can be used to explain its effect on the surface energy of the Ag_3Sn crystal. It is known that larger surface tension correlates with faster plane growth and greater adsorption of surface-active materials [12,18].

3.2. The top morphology of the IMC layer

To demonstrate further, Fig. 5a–d presents the top views of the Cu_6Sn_5 IMC layer at the interfaces of the SAC solder joints on Cu substrate after aging for 7 days at different temperatures, followed by etching to remove the solder. It is clear that scallop-type grains, Cu_6Sn_5 grains with a size of 4.4 ± 0.36 μm, formed at the interface soldered at 100 °C for 7 days (Fig. 4a). These scallops appear rounded, and deep channels are visible between them. The hexagonal-type grains after isothermal aging at temperatures over 175 °C can be seen in Fig. 5d. A similar result was also reported by Yoon and Jung [19]. They studied IMC growth with increasing aging times and aging temperature. In addition, the surfaces of the Cu_6Sn_5 grains at the SAC solder/Cu interface had a few seed-type particles (mark a), and were embedded with the Cu_6Sn_5 grains, as shown in Fig. 5a. The Cu_6Sn_5 grain surface shown in Fig. 5d was then used to obtain the X-ray diffraction patterns of Cu_6Sn_5 and Ag_3Sn grains. However, the inner Cu_3Sn layer was not observed (Fig. 5e). The lead-free solders on top of the joints have been etched away with unreacted solder. This indicates that the seed-type IMC were Ag_3Sn. This observation is consistent with a previous study on the intermetallic growth in the Sn3.5Ag/Cu [20,21] and Sn3.5Ag0.7Cu/Cu interface after aging [19]. At short times, seed-type Ag_3Sn particles were present in both the Cu_6Sn_5 IMC and in the solder matrix. As the aging times and temperatures increased, the seed-type Ag_3Sn particles grew and became embedded in the Cu_6Sn_5 IMC, as shown in Fig. 5d. The X-ray diffraction pattern of Fig. 5d is shown as Fig. 5e. From SEM and XRD analysis, the seed-type particles were confirmed to be Ag_3Sn, which effectively suppressed the growth of the Cu_6Sn_5 grains.

Fig. 6a–d presents the top views of the Cu_6Sn_5 IMC layer at SAC composite solder/Cu interfaces after aging for 7 days at different temperatures, followed by etching away of the solder. It can be seen that all of the Cu_6Sn_5 IMC changed from scallop-type to hexagonal-type, and the size of the IMC increased with prolonged aging times and increased aging temperature (Fig. 6a–d). It is interesting that the surfaces of the Cu_6Sn_5 grains held no seed-type Ag_3Sn grains. However, the surfaces of the Cu_6Sn_5 grains at the SAC composite solder/Cu interface were rough, and light-colored nanoparticles

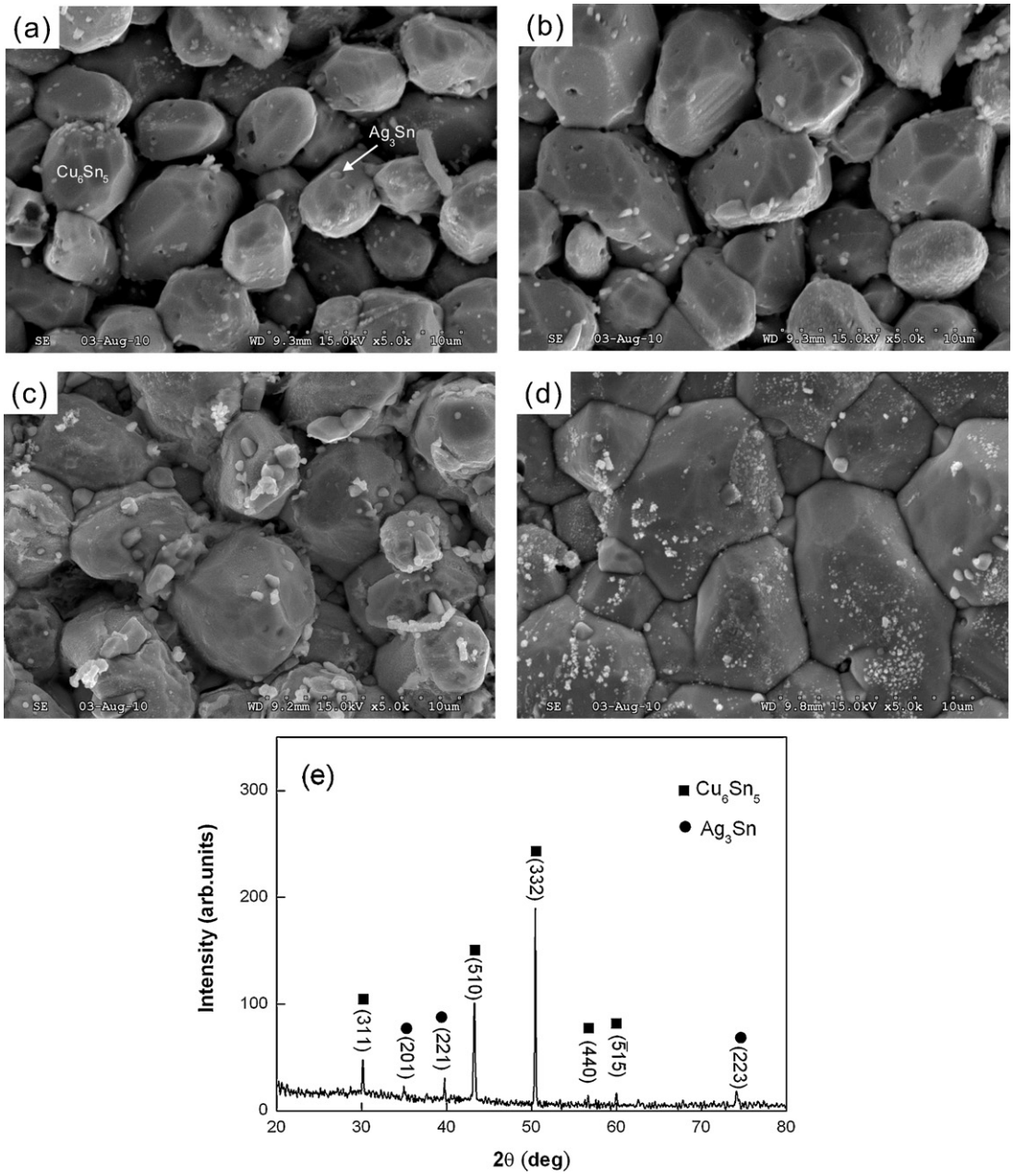

Fig. 5. Top view SEM micrographs of SAC solder/Cu substrate after aging for 7 days at: (a) 100 °C; (b) 125 °C; (c) 150 °C; (d) 175 °C; and (e) X-ray diffraction pattern of (d).

were visible on the surface, as shown in Fig. 6d. The X-ray diffraction pattern of Fig. 6d is shown as Fig. 6e. Comparison of Figs. 5e and 6e reveals some light-colored nano-particles, which were estimated to be nano-Ag_3Sn particles with an average size of 82 ± 6 nm. The grain size of nano-Ag_3Sn particles increased with both prolonged aging time and increased aging temperature. With a short time and low temperature, nano-Ag_3Sn particles were absorbed on the Cu_6Sn_5 surface. With greater aging times and temperatures, the

Table 1
Summary of observed the quantity of Ag_3Sn IMC, calculated diffusion coefficient and activation energy of overall IMCs for SAC composite solder/Cu reaction couples during isothermal aging.

Reactive couples	Temperature (°C)	Capture quantity	Diffusion coefficient, D ($\times 10^{-18}$ m^2/s)	Diffusion constant, D_0 (m^2/s)	Activation energy, Q (kJ/mol)
SAC	100	Ten	4.1981	3.25×10^{-12}	42.48
	125	Ten	6.3555		
	150	Ten	21.6121		
	175	Ten	36.0865		
SAC–0.5TiO_2	100	Million	0.79929	2.53×10^{-10}	60.31
	125	Million	3.20224		
	150	Million	12.5250		
	175	Million	18.3054		

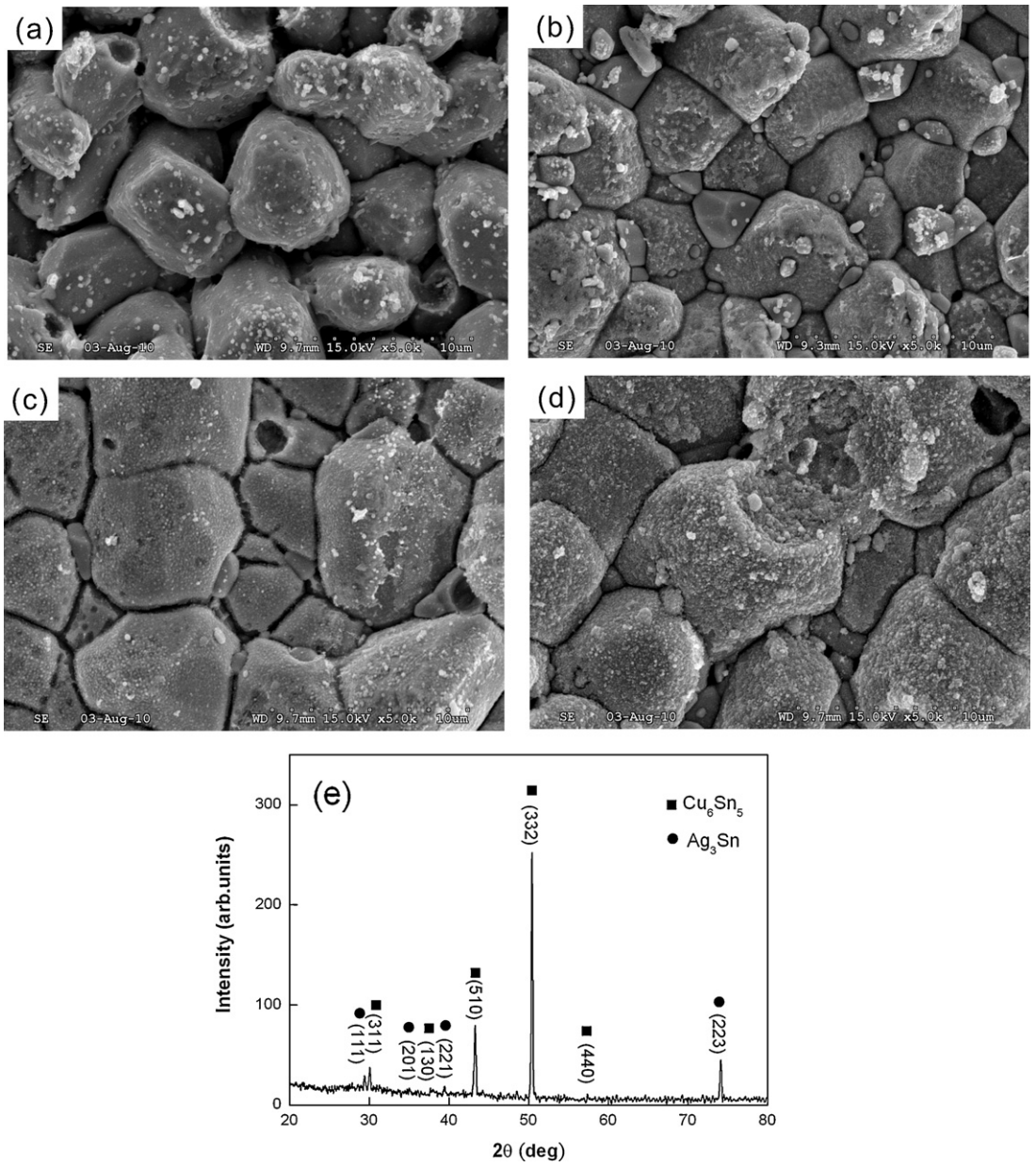

Fig. 6. Top view SEM micrographs of SAC composite solder/Cu substrate after aging for 7 days at: (a) 100 °C; (b) 125 °C; (c) 150 °C; (d) 175 °C; and (e) X-ray diffraction pattern of (d).

adsorbed nano-Ag_3Sn particles became a moss-type layer on the Cu_6Sn_5 surface. Comparing the two joints, the adsorption amount, moss-type condition, and nano-size of Ag_3Sn particles in the SAC composite solder joint exceed those of the SAC solder joint (Table 1). Also, the XRD pattern of the SAC composite solder/Cu indicates the additional presence of a new Ag_3Sn peak ($2\theta = 29.34^\circ$). From SEM and XRD analysis, we determined that the addition of nano-TiO_2 particles in SAC composite solder/Cu joints affects the absorbed nano-Ag_3Sn particles. This observation is consistent with the suggestion above that Sn diffuses through the nano-Ag_3Sn IMC layer to react with the Cu substrate.

Zhao et al. [22] reported that that the critical grain size at which the adsorption behavior of Ag_3Sn particles on a Cu_6Sn_5 surface occurs is about 2 μm. Yu et al. [18] have reported finding nano-size Ag_3Sn particles on a varying IMC surface. The existence of these nanoparticles would decrease the interfacial energy and suppress the growth of the IMC layer. Liu et al. [23] have found that the adsorption of Ag_3Sn particles occurs during the solidification process, and that the number of nano-Ag_3Sn particles increases with the changes in morphology of the Cu_6Sn_5 IMC. In a previous study, the morphology of Cu_6Sn_5 grains was shown to be affected by adsorption of nano-Ag_3Sn particles. Especially, the scallop-type Cu_6Sn_5 grains formed by the ripening process are likely to be "captured" by the large amount of nano-Ag_3Sn particles. Also, the adsorption will decrease the surface energy of the Cu_6Sn_5 compounds and retard the growth of the whole IMC layer [18]. Gibbs adsorption theory is used to explain the formation of these particles and their effect on the surface energy of the IMC [12,18,23].

According to the Gibbs adsorption equation, the adsorption amount of active material (nano-Ag_3Sn particles) at the crystal plane K (Cu_6Sn_5 grain) [12] is

$$\Gamma^K = -\frac{C}{RT}\frac{d\gamma^K}{dC} \tag{2}$$

where Γ^K is the adsorption of surface-active material at crystal plane K, C is the total concentration of the active material, R is

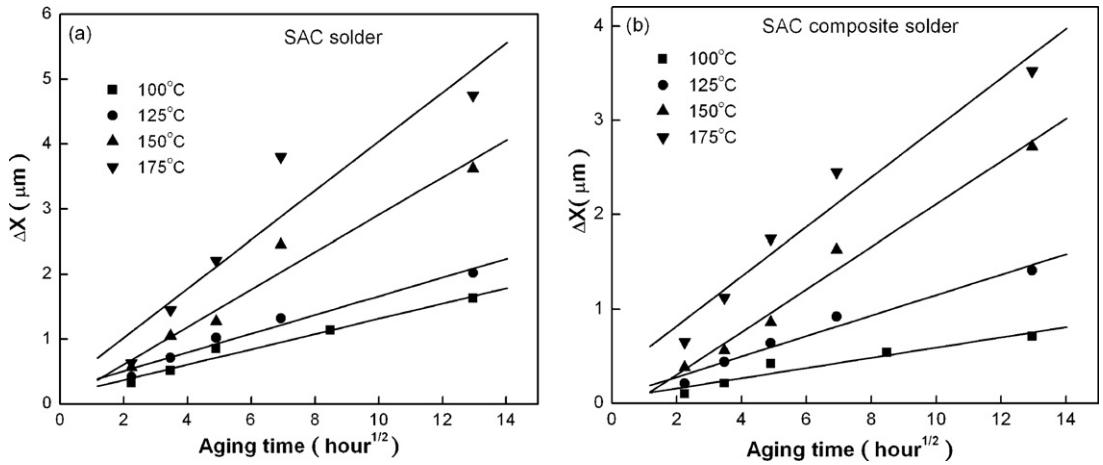

Fig. 7. The relationship curves between IMC thickness, aging temperature, and aging time ($h^{1/2}$) for SAC solder/Cu (a) and SAC composite solder/Cu (b) during isothermal aging.

the Plank constant, T is the absolute temperature, and γ^K is the surface tension of the crystal plane K. Generally, the crystal plane with maximum surface tension grows the fastest, while its adsorption amount of surface-active material is maximized. However, an increase in adsorption elements decreases its surface energy and, therefore, decreases the growth velocity of this crystal plane. First, the adsorption of nano-TiO_2 particles will decrease the surface energy of the primary Ag_3Sn crystal. Hence, the nano-TiO_2 particles refine the Ag_3Sn IMC particles. Second, compared with the Cu_6Sn_5 IMC, nano-Ag_3Sn particles are very small in the SAC composite solder/Cu. As a result, they are regarded as effective surface-active agents, which may be adsorbed on the surface of the IMC particles and suppress excessive growth. Therefore, this entire interface would capture the nano-Ag_3Sn particles preferentially; Gibbs tells us that the surface energy is reduced, and this reduction will decrease the growth velocity of the Cu_6Sn_5 grains. It has always been quite difficult to calculate the surface energy in order to minimize the free energy of the entire interface in SAC composite solder/Cu substrate. Hence, there is no doubt that this plane will capture a large amount of the nano-Ag_3Sn particles formed on the scallop-type Cu_6Sn_5 IMC layer, which could reduce the interfacial energy during solidification. Moreover, the composite solder joints were also effective in retarding the growth of the Cu_6Sn_5 IMC layer.

3.3. Kinetic energy of IMC layer

3.3.1. Theory of kinetic energy

The kinetics of IMC growth can be diffusion-controlled or interfacial-reaction controlled [24,25]. In Fig. 7, the mean thickness of the overall IMC layer ($Cu_6Sn_5 + Cu_3Sn$) is plotted as a function of aging time and temperature, showing that the overall IMC thickness increases monotonically with aging time and grows faster at higher aging temperature. It is interesting that the overall IMC growth for the SAC composite solder/Cu is extremely depressed during solid-state aging. The curve indicates that the IMC growth corresponds with a diffusion-controlled reaction; that is, the IMC thickness during isothermal aging follows the linear relationship with the square root of aging time. This process can be described by the empirical diffusion formula and the Arrhenius equation as follows:

$$X_t = X_0 + \sqrt{Dt} \tag{3}$$

$$D = D_0 \exp\left(\frac{-Q}{RT}\right) \tag{4}$$

where X_t is the IMC thickness (m) at aging time t (s), X_0 is the initial thickness (m) after reflowing, and D is the diffusion coefficient (m^2/s). D_0 is the diffusion constant (m^2/s), Q is the activation energy (kJ/mol), R is the gas constant, and T is the absolute temperature (K). Fig. 8 represents the Arrhenius plot, which is obtained based on the data in Fig. 7 for SAC solder/Cu and SAC composite/Cu, respectively. The diffusion coefficients, D, for growth of the overall IMC layer in the SAC solder and SAC composite solder joints at different aging temperatures are displayed in Table 1. From Eq. (4) and the data in Fig. 8, the diffusion constants were calculated to be 3.25×10^{-12} and 2.53×10^{-10} m^2/s for SAC and SAC composite solders, respectively. The activation energies for the growth of the interfacial overall IMC layer during the solid-state aging process are estimated to be 42.48 kJ/mol for SAC solder/Cu and 60.31 kJ/mol for SAC composite solder/Cu. The high activation energy of the overall IMC layer in the SAC composite solder/Cu joints resulted from the low growth rate constants at low aging temperatures and the high growth rate constants at high aging temperatures, because the activation energy is obtained from the temperature dependence of the diffusion coefficient, D. As is well known, the Cu_6Sn_5 grains were first formed during the interfacial reaction between Sn and Cu substrate, and then another Cu_3Sn IMC would form between the Cu_6Sn_5 layer and Cu substrate with increasing reflow time or aging time [26–28].

As in the experiment above, the overall IMC growth is a diffusion-controlled reaction that occurs during the isothermal aging process. Thus, the typical growth of Cu_6Sn_5 and Cu_3Sn phases

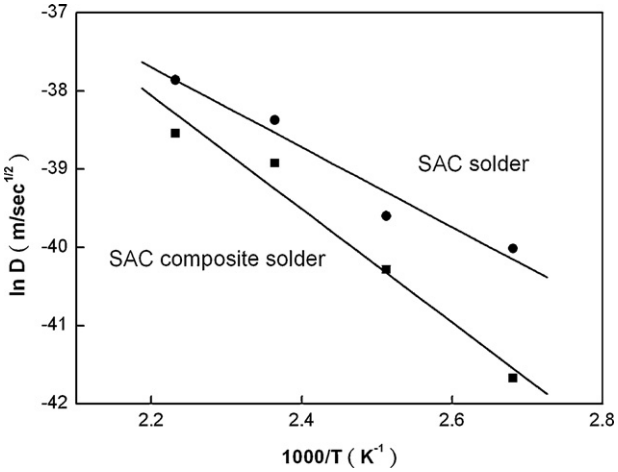

Fig. 8. Arrhenius plot of overall IMC layer formed by SAC solder/Cu and SAC composite solder/Cu.

relies on the interdiffusion coefficient of Cu and Sn atoms, or the diffusion flux of Sn atoms from the solder matrix to the solder/Cu_6Sn_5 interface and flux of Cu atoms from Cu substrate to solder/Cu_6Sn_5 or Cu_6Sn_5/Cu_3Sn interface [29]. This diffusion mechanism was directly observed in a previous TEM study of the Sn–Pb solder system [30].

However, in the SAC composite solder/Cu joints, except for the typical growth of the overall IMC mechanism, there is an added new diffusion flux interface, the diffusion flux of Sn atoms from the solder matrix to the solder/Ag_3Sn/Cu_6Sn_5 interface, and the flux of Cu atoms from Cu substrate to the solder/Ag_3Sn/Cu_6Sn_5 or Ag_3Sn/Cu_6Sn_5/Cu_3Sn interface. This suggests that the significantly depressed growth of the overall IMC layer in the SAC composite solder/Cu joint can be attributed to the effect of nano-Ag_3Sn particle adsorption on the surface of Cu_6Sn_5 grains on the migration of Sn atoms toward the solder/Ag_3Sn/overall IMC interface. The results in Table 1 also indicate that the diffusion coefficients for SAC composite solder/Cu are always smaller than those for SAC solder/Cu at any aging temperature. The presence of 0.5 wt.% nano-TiO_2 particles in the solder can increase the adsorption of nano-Ag_3Sn particles on the surface of Cu_6Sn_5 grains, and then may decrease the activity of Sn atoms; thus, in turn, the necessary energy for the migration of Sn atoms from the solder to the solder/Ag_3Sn/overall IMC interface may increase. On the other hand, the diffusion of Cu atoms toward the solder/Ag_3Sn/Cu_6Sn_5 or solder/Ag_3Sn/Cu_6Sn_5/Cu_3Sn IMC interface is not affected due to the absence of nano-Ag_3Sn particles or nano-TiO_2 particles in the IMC.

Wang et al. [29] reported that the IMC growth was remarkably suppressed by the addition of 0.2 wt.% Zn to the SAC solder matrix, and this effect tended to be more prominent at higher aging temperatures. Many studies have reported that nano-sized, nonreacting, noncoarsening oxide dispersoid particles, such as TiO_2, Y_2O_3, CNTs, and ZrO_2, can affect the growth rate of interfacial IMC. In other words, there exists a stronger affinity of Ag and Sn in the case of nano-TiO_2 addition into the SAC solder, which increases the precipitation or adsorption of Ag_3Sn nanoparticles.

The growth of the overall IMC layer in composite solder joints was lower at the temperature used in this study than in joints of SAC solder. This suggests that the addition of nano-TiO_2 particles to the SAC solder can increase the adsorption of nano-Ag_3Sn particles on Cu_6Sn_5 IMC grains, effectively suppressing the growth of the overall IMC layer. This is consistent with the studies by other investigators [31–33].

4. Conclusions

The study detailed the microstructural evolution and growth kinetics of the IMC layer in the SAC solder/Cu and SAC composite solder/Cu interface during aging at temperatures ranging from 100 °C and 175 °C for up to 7 days.

In the SAC solder/Cu joints, a few coarse Ag_3Sn particles were embedded in the Cu_6Sn_5 surface and grew with prolonged aging time. However, in the SAC composite solder/Cu joints, numerous nano-Ag_3Sn particles were adsorbed onto the Cu_6Sn_5 surface. The morphology of the adsorbed nano-Ag_3Sn particles changed dramatically from adsorption-type to moss-type, and the size of the particles increased. Based on Arrhenius plots, the activation energies of overall IMC layer growth were calculated as 42.48 kJ/mol and 60.31 kJ/mol for the SAC solder and SAC composite solder joints, respectively. The reduced diffusion coefficient was confirmed for the SAC composite solder/Cu joints.

Acknowledgment

The authors acknowledge the financial support of this work from the National Science Council of the Republic of China under Project No. NSC97-2218-E-020-004.

References

[1] I. Anderson, J. Mater. Sci.: Mater. Electron. 18 (2007) 55–76.
[2] J. Glazer, J. Electron. Mater. 23 (1994) 693–700.
[3] J.W. Yoon, B.I. Noh, B.K. Kim, C.C. Shur, S.B. Jung, J. Alloys Compd. 486 (2009) 142–147.
[4] Y.Y. Shiue, T.H. Chuang, J. Alloys Compd. 491 (2010) 610–617.
[5] G. Ghosh, Acta Mater. 48 (2000) 3719–3738.
[6] X. Ma, F. Wang, Y. Qian, F. Yoshida, Mater. Lett. 57 (2003) 3361–3365.
[7] W. Yang, L.E. Feltion, R.W. Messler, J. Electron. Mater. 24 (1995) 1465–1472.
[8] T.H. Chuang, M.W. Wu, S.Y. Chang, C.C. Ping, L.C. Tsao, J. Mater. Sci.: Mater. Electron. (2010), doi:10.1007/s10854-010-0253-1.
[9] A.K. Gain, T. Fouzder, Y.C. Chan, A. Sharif, N.B. Wong, W.K.C. Yung, J. Alloys Compd. 506 (2010) 216–223.
[10] L.C. Tsao, S.Y. Chuang, Mater. Des. 31 (2010) 990–993.
[11] L.C. Tsao, S.Y. Chang, C.I. Lee, W.H. Sun, C.H. Huang, Mater. Des. 31 (2010) 4831–4835.
[12] L.C. Tsao, J. Alloys Compd. 509 (2011) 2326–2333.
[13] L.C. Tsao, C.P. Chu, S.F. Peng, Microelectron. Eng. (2011) 034, doi:10.1016/j.mee.2011.04.
[14] J. Shen, Y.C. Liu, Y.J. Han, Y.M. Tian, H.X. Gao, J. Electron. Mater. 35 (2006) 1672–1679.
[15] C.W. Hwang, J.G. Lee, K. Suganuma, H. Mori, J. Electron. Mater. 32 (2003) 52–62.
[16] K.N. Tu, R.D. Thompson, Acta Metall. 30 (1982) 947–952.
[17] H. Hao, Y. Shi, Z. Xia, Y. Lei, F. Guo, J. Electron. Mater. 37 (2008) 2–8.
[18] D.Q. Yu, L. Wang, C.L. Wu, C.M.T. Law, J. Alloys Compd. 389 (2005) 153–158.
[19] J.W. Yoon, S.B. Jung, J. Mater. Sci. 39 (2004) 4211–4217.
[20] D.R. Flanders, E.G. Jacobs, R.F. Pinizzotto, J. Electron. Mater. 26 (1997) 883–887.
[21] S. Choi, T.R. Bieler, J.P. Lucas, K.N. Subramanian, J. Electron. Mater. 28 (1999) 1209–1215.
[22] N. Zhao, X.M. Pan, H.T. Ma, C. Dong, S.H. Guo, W. Lu, L. Wang, Phys.: Conf. Ser. 98 (2008) 012029.
[23] X.Y. Liu, M.L. Huang, Y.H. Zhao, C.M.L. Wu, L. Wan, J. Alloys Compd. 492 (2010) 433–438.
[24] J.W. Jang, P.G. Kim, K.N. Tu, D.R. Frear, P. Thompson, J. Appl. Phys. 85 (1999) 8456–8463.
[25] K. Jung, H. Conrad, J. Electron. Mater. 30 (2001) 1308–1312.
[26] T.Y. Lee, W.J. Choi, K.N. Tu, J.W. Jang, S.M. Kuo, J.K. Lin, D.R. Frear, K. Zeng, J.K. Kivilahti, J. Mater. Res. 17 (2002) 291–301.
[27] T. Lauril, V. Vuorinen, J.K. Kivilahti, Mater. Sci. Eng. Rep. 49 (2005) 1–60.
[28] Q.S. Zhu, Z.F. Zhang, J.K. Shang, Z.G. Wang, Mater. Sci. Eng. A 435–436 (2006) 588–594.
[29] F.J. Wang, F. Gao, X. Ma, Y.Y. Qian, J. Electron. Mater. 35 (2006) 1818–1824.
[30] Y. Wu, J.A. Sees, C. Pouraghabagher, L.A. Foster, J.L. Marshall, E.G. Jacobs, R.F. Pinizzotto, J. Electron. Mater. 22 (1993) 769–777.
[31] T. Fouzder, I. Shafiq, Y.C. Chan, A. Sharif, W.K.C. Yung, J. Alloys Compd. 509 (2011) 1885–1892.
[32] A.K. Gain, T. Fouzder, Y.C. Chan, W.K.C. Yung, J. Alloys Compd. 509 (2011) 3319–3325.
[33] L.C. Tsao, C.P. Chu, S.F. Peng, Microelectron. Eng. (2011) doi:10.1016/j.mee.2011.04.034.